

VORTEX-ANTIVORTEX PAIR DYNAMICS IN THE PRESENCE OF AN IMMOBILE VORTEX IN TWO-DIMENSIONAL FERROMAGNET

V.P. KRAVCHUK

PACS 75.75.+a, 75.70.Ak,
75.10.Hk
©2010

Bogolyubov Institute for Theoretical Physics, Nat. Acad. of Sci. of Ukraine
(14b, Metrolohichna Str., Kyiv 03680)

The dynamics of a vortex-antivortex pair in the presence of an immobile vortex in a two-dimensional ferromagnet is theoretically studied. The calculations are performed within the model of collective variables. Criteria for the initial conditions allowing one to separate the finite and infinite motions of the pair are obtained. General characteristics of each of the types of motion are described.

1. Introduction

One of the main reasons for a significant increasing interest in magnetic vortices which is observed now in the physics of nanomagnets is the possibility to use nanomagnets as bits of information for the energy-independent memory in computers (MRAM – Magnetic Random Access Memory) [1, 2]. As nanomagnets, it is accepted to call particles of a magnetic material with submicronic sizes. Experimental studies are carried out most frequently with quasi-two-dimensional magnetics, whose thickness does not exceed several tens of nanometers. Thus, a particle is sufficiently small in order that its magnetization be considered invariable through its thickness. An attracting specific feature of nanomagnets consists in that the minimum of their magnetic energy corresponds to an essentially inhomogeneous distribution of their magnetization, whose specific shape is determined by the competition between the exchange and nonlocal magnetostatic interactions. As a result, the magnetization distribution is very sensitive to the shape and size of a particle. In this case, the characteristic size of inhomogeneities is $\ell = \sqrt{A/(4\pi M_s^2)}$, where A is the exchange interaction constant, M_s is the magnetic moment per unit volume in the saturation state. For most magnets, $\ell = 5 - 10$ nm [3]. For particles of symmetric shapes such as nanodisks, nanorings, and regular prisms, the vortex distribution of magnetization turns out often to be most energy-gained [4–8]:

$$\cos \theta = pf(r), \quad \varphi = q\chi + \varphi_0. \quad (1)$$

Here and below, we use a cylindrical coordinate system (r, χ, z) , whose axis z is directed normally to the plane of a magnet. To describe the distribution of a magnetization $\mathbf{M}(\mathbf{r})$, we use the angular variables $\theta(\mathbf{r})$ and $\varphi(\mathbf{r})$ which are defined in the following way: $\mathbf{M} = M_s(\sin \theta \cos \varphi, \sin \theta \sin \varphi, \cos \theta)$. The function f is localized near the vortex center ($r = 0$) and is such that $f(0) = 1$, $f(\infty) = 0$. The region of localization of the function f has a characteristic size ℓ and is called the vortex core. The quantity $p = \pm 1$ is called the vortex polarity. The vorticity q is an integer and is equal to the number of full turns of the magnetization vector at the bypass around the vortex center. If q is negative, distribution (1) is conditionally called an antivortex.

The polarity of a vortex p is a promising candidate to store a bit of information [9, 10]. In the continuous model of a magnetic medium, the value of p is a topological invariant and cannot be changed by external factors. However, in a real magnetic crystal which is a discrete system, the polarity p remaining stable to the random external factors can be switched in a controlled manner [9, 11]. All available methods to switch the polarity of a vortex [12–17] are realized through the intermediate process of creation of a vortex-antivortex pair with polarities opposite to the polarity of the initial vortex. In this case, two types of the dynamics which depend on the position of the initial vortex and the new created pair are possible: (i) a new antivortex is captured by the initial vortex, approaches it due to the damping, and annihilates. As a result, only a new vortex with opposite polarity remains. This mechanism presents the essence of the switching of the vortex polarity. (ii) The new vortex-antivortex pair performs a fast quasicollinear movement, goes far away from the initial vortex, and self-annihilates. In this case, no switching occurs. The question about the determination of conditions, under which a certain mechanism is realized, is open and actual. The purpose of the present work is to find an evaluation criterion for the initial con-

ditions which would allow one to separate two indicated mechanisms.

2. Model. Equations of Motion

The statics and the dynamics of inhomogeneous distributions of magnetization are traditionally described by the Landau–Lifshitz phenomenological equation [18] which has the following form in terms of the angular variables [19]:

$$\sin \theta \dot{\theta} = -\frac{\delta \mathcal{E}}{\delta \varphi}, \quad \sin \theta \dot{\varphi} = \frac{\delta \mathcal{E}}{\delta \theta}. \quad (2)$$

Here and below, we measure the time in the units $\tau = 1/\omega_0$, where $\omega_0 = 4\pi\gamma M_s$, and $\gamma = g|e|/(2mc)$ is the gyromagnetic ratio; for most magnets, $\tau = 10 - 50$ ps; $\mathcal{E} = E/(4\pi M_s^2)$, where E is the total magnetic energy of a magnet. One of the possible static solutions of Eqs. (2) for an easy-plane magnetic is the vortex distribution (1) [19]. In this case, the role of effective easy-plane anisotropy for quasi-two-dimensional magnetics can be played by the magnetostatic interaction [20].

In what follows, the dynamics of a magnetic vortex (antivortex) will be described within the approximate *method of collective variables* [21, 22], where the dynamics of the magnetization field $[\theta(\mathbf{r}, t), \varphi(\mathbf{r}, t)]$, which is a system with the infinite number of degrees of freedom, is approximately described by a finite number of collective variables. In the simplest case, we can choose the coordinates of the vortex center as such collective variables. In this case, it is assumed that the vortex moves as a whole, without any change in its shape. Within such an approach, the equation of motion (2) takes the form of the Thiele equation [23, 24]

$$[\mathbf{G} \times \dot{\mathbf{R}}] + \mathbf{F} = 0, \quad (3)$$

where the radius-vector $\mathbf{R}(t)$ gives a position of the vortex center. The gyrovector $\mathbf{G} = \int \mathbf{g} d^3\mathbf{r}$, where the gyrodensity $\mathbf{g}(\mathbf{r}) = [\nabla(\cos \theta) \times \nabla \varphi]$. For the vortex distribution (1), $\mathbf{G} = -2\pi h p q \hat{\mathbf{z}}$ [24], where h is the thickness of a magnetic, and $\hat{\mathbf{z}}$ is the unit vector along the axis z . The effective force $\mathbf{F} = -d\mathcal{E}/d\mathbf{R}$ can be induced by the action of an external field, the effect of a surface, the inhomogeneous distribution of material parameters in a specimen, or by the interaction with other vortices. If the distances between vortices in a magnetic are sufficiently large, so that their out-of-plane components ($\cos \theta$) do not overlap, then the force acting on the i -th vortex from the

side of all other vortices is determined as [24]

$$\mathbf{F}_i = 2\pi\ell^2 h q_i \sum_{j \neq i} q_j \frac{\mathbf{R}_i - \mathbf{R}_j}{|\mathbf{R}_i - \mathbf{R}_j|^2}. \quad (4)$$

The problem posed in the previous section is solved in the frame of the following model: (i) Let us consider a quasi-two-dimensional ferromagnetic plate with infinite size which contains an immobile vortex (IV); for example, a vortex pinned by an impurity. The same plate contains a vortex (V) and antivortex (AV) with identical polarity $p = +1$ and with $|q| = 1$, whose motion is not artificially limited. (ii) It is assumed that the out-of-plane components of V and AV do not overlap each other at their motion. That is, the distribution of gyrodensity in the system is given by $\mathbf{g}(\mathbf{r}) = -2\pi h [\delta(\mathbf{r} - \mathbf{R}_v) - \delta(\mathbf{r} - \mathbf{R}_a)]$, where the radius-vectors \mathbf{R}_v and \mathbf{R}_a determine the positions of V and AV, respectively. (iii) Interaction (4) is unique in the system. (iv) Damping is absent.

The above-described model can be applied only in the case where the distance d between V and AV is large ($d \gg \ell$), which justifies the assumption that their out-of-plane components do not overlap each other. The description of the interaction of a V–AV pair at small distances was recently given in [25, 26] on the basis of numerical calculations.

Within our model, the equations of motion (3) for V and AV take the form

$$\begin{aligned} \frac{\mathbf{R}_v}{R_v} + [\dot{\mathbf{R}}_v \times \hat{\mathbf{z}}] + \frac{\mathbf{R}_a - \mathbf{R}_v}{|\mathbf{R}_a - \mathbf{R}_v|^2} &= 0, \\ -\frac{\mathbf{R}_a}{R_a} - [\dot{\mathbf{R}}_a \times \hat{\mathbf{z}}] + \frac{\mathbf{R}_v - \mathbf{R}_a}{|\mathbf{R}_v - \mathbf{R}_a|^2} &= 0. \end{aligned} \quad (5)$$

Here and below, the distances are measured in units ℓ , and the coordinate system origin is located at IV.

We denote $\mathbf{R}_i = R_i(\cos \Phi_i, \sin \Phi_i, 0)$, where $i = a, v$. By introducing the variable $\Psi = \Phi_a - \Phi_v$, we reduce the system of four equations (5) to a system of three equations

$$\begin{aligned} \dot{\Psi} &= \frac{R_a^2 - R_v^2 + R_a R_v \cos \Psi}{R_a^2 R_v^2} - 2 \frac{\sin^2 \Psi}{|\mathbf{R}_v - \mathbf{R}_a|^2}, \\ \dot{R}_v &= \frac{R_a \sin \Psi}{|\mathbf{R}_v - \mathbf{R}_a|^2}, \quad \dot{R}_a = \frac{R_v \sin \Psi}{|\mathbf{R}_v - \mathbf{R}_a|^2}. \end{aligned} \quad (6)$$

2.1. Stationary solutions

It is easy to see that system (6) has two stationary solutions: (i) ($\Psi = 0$, $R_a/R_v = \gamma$) and (ii) ($\Psi = \pi$, $R_a/R_v = \bar{\gamma}$), where we introduce the notation $\gamma = (\sqrt{5} - 1)/2$, $\bar{\gamma} = (\sqrt{5} + 1)/2$.

Substituting the first of these solutions to the initial system (5), we obtain $\dot{\Phi}_v = \dot{\Phi}_a = \gamma/R_a^2 = \bar{\gamma}/R_v^2 = \Omega_1$. Analogously, for the second solution, $\Omega_2 = -\bar{\gamma}R_a^2 = -\gamma R_v^2$. The first solution means that if IV, AV, and V are positioned on a single straight line at the initial time moment so that AV divides the segment IV-V by the *golden section*, being closer to V, then such a system uniformly rotates around IV with constant frequency Ω_1 . This dynamics is illustrated in Fig. 1, *a*. The interpretation of the second solution is analogous: if V, IV, and AV are positioned on a single straight line at the initial time moment so that IV divides the segment V-AV by the *golden section*, being closer to V, then the whole system uniformly rotates around IV with frequency Ω_2 (see Fig. 1, *b*).

The analysis for the stability by Lyapunov indicates that both mentioned stationary solutions are saddles, i.e. the solutions are unstable.

3. Integrals of Motion. Different Types of the Dynamics

By dividing two last equations of system (6) by each other, we obtain $\dot{R}_v/\dot{R}_a = R_a/R_v$. This yields $\frac{d}{dt}(R_v^2 - R_a^2) = 0$, i.e. we have shown the conservation of the quantity

$$L = R_v^2 - R_a^2 \quad (7)$$

which has sense of the angular momentum [25–27]. Once more integral of motion is the energy. In view of interactions (4), it has form $\mathcal{E} = \ln \frac{R_v}{R_a|\mathbf{R}_a - \mathbf{R}_v|}$ [24]. We can easily verify the formula $\dot{\mathcal{E}} = 0$, by carrying out the direct differentiation with the use of (6). But it is more convenient to use another conserved quantity:

$$E = e^{2\mathcal{E}} = \frac{R_v^2}{R_a^2(R_v^2 + R_a^2 - 2R_v R_a \cos \Psi)}. \quad (8)$$

For simplicity, we also call the quantity E the energy. At once, it is worth to note that $E > 0$ in all cases.

The form of the integrals of motion (7) and (8) allows us to make a few conclusions: (i) due to the conservation of quantity (7), the motion of *both* particles V and AV should be finite or infinite. That is, the situation where one particle realizes a finite motion, whereas the motion

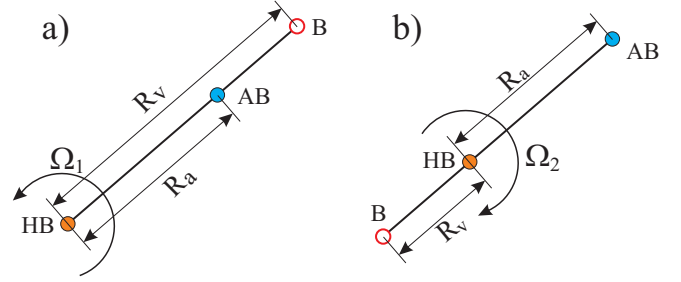


Fig. 1. Stationary solutions of system (6): *a*) $\Psi = 0$, *b*) $\Psi = \pi$

of another one is infinite, is impossible. (ii) At the infinite motion, $R_v/R_a \rightarrow 1$. In this case, (iii) the distance d between V and AV tends to a constant $d \rightarrow 1/\sqrt{E}$.

Possessing two integrals of motion (7) and (8), we can pass from the system of three equations (6) to a single equation. For the quantity R_v , such an equation has form

$$\begin{aligned} \dot{R}_v^2 = & \left[4ER_v^6 - (E^2L^2 + 6EL + 1)R_v^4 + \right. \\ & \left. + 2EL^2(EL + 1)R_v^2 - E^2L^4 \right] / (4R_v^6), \end{aligned} \quad (9)$$

and the quantity R_a obeys the equation

$$\begin{aligned} \dot{R}_a^2 = & \left[4ER_a^6 - (E^2L^2 - 6EL + 1)R_a^4 + \right. \\ & \left. + 2L(EL - 1)R_a^2 - L^2 \right] / [4R_a^2(L + R_a^2)^2]. \end{aligned} \quad (10)$$

The relevant equation for Ψ has form too awkward for the analysis, and we will not consider it. It is sufficient to solve one of Eqs. (9) and (10). In this case, the solution of another equation follows automatically from (7). However, to ensure the symmetry of calculations and the clearness, we will analyze both indicated equations (9) and (10) simultaneously.

First, we consider the simplest partial case where $L = 0$. This means that $R_v = R_a = R$, and, by virtue of the conservation of the quantity L , this equality remains true at any time moment of the dynamics. In this case, energy (8) takes form $E = 1/[2R^2(1 - \cos \Psi)] = 1/d^2$, where d is the distance between V and AV. The conservation of the quantity E means that the distance between V and AV does not vary during the dynamical process and is equal to $d = 1/\sqrt{E}$. In the case under consideration, system (6) can be easily solved:

$$R = R_0 \frac{\cos \Psi_0/2}{\cos \Psi/2}, \quad \text{ctg} \frac{\Psi}{2} = \text{ctg} \frac{\Psi_0}{2} + 2Et, \quad (11)$$

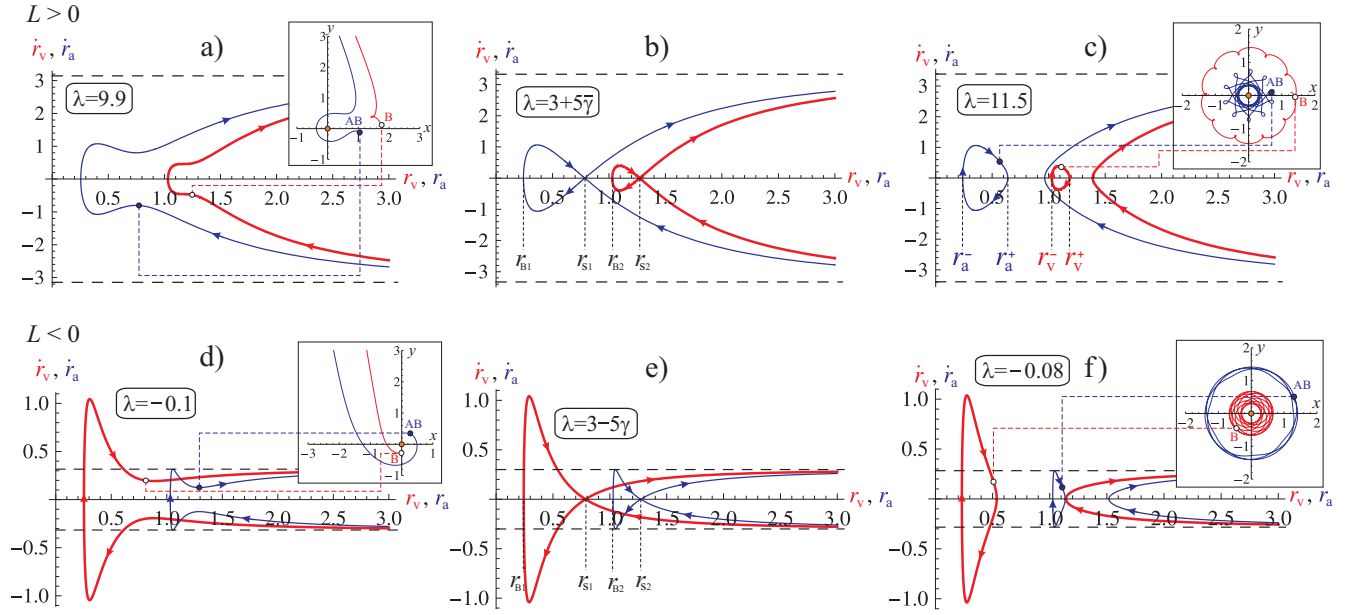


Fig. 2. Dependences $\dot{r}_v(r_v)$ (thick lines) and $\dot{r}_a(r_a)$ (thin lines) for various values of the parameter λ . The upper row (a, b, c) shows dependences (14) corresponding to positive λ , and the lower row (d, e, f) corresponds to negative λ . The inserts give the examples of possible trajectories of the V–AV pair for a given value of λ . The black and white points indicate the initial positions of AV and V, respectively. The trajectories are constructed as a direct numerical solution of Eqs. (5); the distances are measured in units l

where we denoted $R_0 = R(t = 0)$, $\Psi_0 = \Psi(t = 0)$. In addition, in the case where $R_v = R_a$, the initial system (5) yields easily the relation $\dot{\Phi}_a = 3\dot{\Phi}_v$. By integrating this relation, we get

$$\Phi_a - \Phi_{a0} = 3(\Phi_v - \Phi_{v0}). \quad (12)$$

Substituting (12) in the first of Eqs. (11) and taking $\Psi = \Phi_a - \Phi_v$ into account, we obtain the trajectory of motion for V and AV:

$$R_v = R_0 \frac{\cos \Psi_0 / 2}{\cos(\Phi_v - \Phi_{v0} + \frac{\Psi_0}{2})},$$

$$R_a = R_0 \frac{\cos \Psi_0 / 2}{\cos(\frac{\Phi_a - \Phi_{a0}}{3} + \frac{\Psi_0}{2})}. \quad (13)$$

As seen, the trajectory of motion of the vortex $R_v(\Phi_v)$ is a straight line. In this case, the motion of the V–AV pair is infinite.

In the general case where $L \neq 0$, by changing the variables $r_v = R_v / \sqrt{|L|}$, $r_a = R_a / \sqrt{|L|}$, $t' = t / |L|$, we succeeded to reduce the number of parameters in Eqs. (9) and (10) to 1:

$$\dot{r}_v^2 = \sigma \frac{4\lambda r_v^6 - \sigma(\lambda^2 + 6\lambda + 1)r_v^4 + 2\lambda(\lambda + 1)r_v^2 - \sigma\lambda^2}{4r_v^6}$$

$$\dot{r}_a^2 = \sigma \frac{4\lambda r_a^6 - \sigma(\lambda^2 - 6\lambda + 1)r_a^4 + 2(\lambda - 1)r_a^2 - \sigma}{4r_a^2(1 + \sigma r_a^2)^2}. \quad (14)$$

Here, $\sigma = \text{sign}(L)$, $\lambda = EL$, and the dot stands for the differentiation with respect to the new time t' . The dependences $\dot{r}_v(r_v)$ and $\dot{r}_a(r_a)$ set in (14) for various values of the parameter λ are shown in Fig. 2. The upper and lower rows correspond to $L > 0$ and $L < 0$, respectively. In the further analysis, the cases with different signs of L will be considered separately.

$L > 0$. This means that $R_v > R_a$, and this inequality is valid at any time moment of the dynamics of the V–AV pair. A simple analysis shows that the critical value of the parameter λ , at which the form of relations (14) changes qualitatively, is equal to $\lambda_{c1} = 3 + 5\gamma$ (see Fig. 2, a–c). At $0 < \lambda < \lambda_{c1}$, the motion of the V–AV pair can be only infinite (Fig. 2, a). At $\lambda > \lambda_{c1}$, there appears a cycle on the dependences $\dot{r}_v(r_v)$ and $\dot{r}_a(r_a)$, which means the possibility of a finite motion (see Fig. 2, c). In this case, the vortex and the antivortex move in the limits of the rings $r_v^-(\lambda) < r_v(t) < r_v^+(\lambda)$ and $r_a^-(\lambda) < r_a(t) < r_a^+(\lambda)$, respectively, and the sizes of these rings decrease with increase in λ (see Fig. 3 for $\lambda > 0$).

The maximally possible values of the quantities r_a and r_v at a finite motion are, respectively, $r_{S1} = \sqrt{\gamma}$ and $r_{S2} = \sqrt{\gamma}$ (see Fig. 3 and Fig. 2, b). The conditions

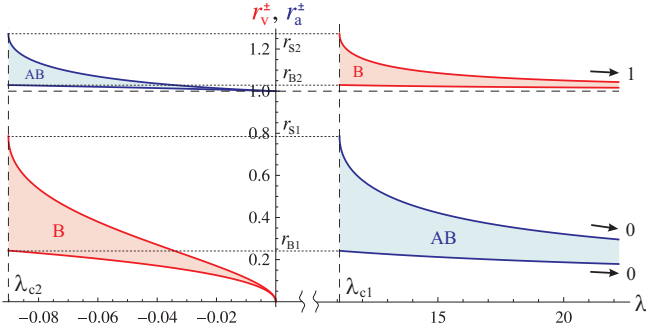


Fig. 3. Sizes of the rings where V (red color) and AV (blue color) move at their finite motion. For the critical values of the parameter λ , these sizes are: $r_{S1} = \sqrt{\gamma}$, $r_{S2} = \sqrt{\bar{\gamma}}$, $r_{B1} = \sqrt{2\gamma - 1}/2$, $r_{B2} = \sqrt{2\bar{\gamma} + 1}/2$

$r_a < r_{S1}$ and $r_v < r_{S2}$ turn out equivalent (see the first consequence of the conservation of L on p. 213) and take the form $R_a < \gamma R_v$ in terms of the variables R_a , R_v . Thus, the condition of the finiteness of the motion of the V–AV pair at $L > 0$ is the simultaneous fulfilment of two conditions

$$\begin{cases} \lambda > \lambda_{c1}, \\ R_a < \gamma R_v. \end{cases} \quad (15)$$

In this case, it is worth noting that if conditions (15) are satisfied at the initial time moment, then they will be satisfied at any time moment of the dynamics.

Since the quantity $\lambda = EL$ can be written through $\rho = R_a/R_v$:

$$\lambda = \frac{1 - \rho^2}{\rho^2 (1 + \rho^2 - 2\rho \cos \Psi)}, \quad (16)$$

it is convenient to show the region $\lambda > \lambda_{c1}$ on the plane (x, y) in length units R_v (this is realized in Fig. 4).

In Fig. 4, the condition $\lambda > \lambda_{c1}$ determines two finite regions bounded by a bold line $\lambda = \lambda_{c1}$, but the condition $R_a < \gamma R_v$ is satisfied only for the region which is positioned to the left from the “saddle point” (shaded in blue).

$L < 0$. That is, $R_v < R_a$, and this equality remains valid at any time moment of the dynamics. In this case, the possibility of a finite motion appears at $\lambda_{c2} < \lambda < 0$, where $\lambda_{c2} = 3 - 5\gamma$ (see Fig. 2, e, f). At $\lambda < \lambda_{c2}$, the motion of the V–AV pair can be only infinite (see Fig. 2, d). Since the sizes of the rings, where V and AV move during a finite motion, decrease with increase in λ (see Fig. 3 for $\lambda < 0$), the conditions $r_a < r_{S2}$ and $r_v < r_{S1}$ can serve the additional condition for the

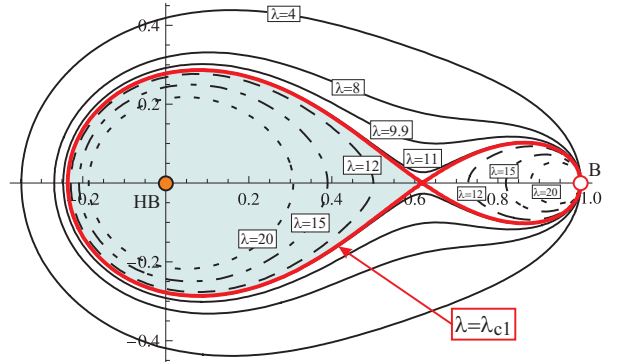


Fig. 4. Ratio $\rho(\Psi)$ given in (16) for various positive values of the parameter λ . If, at a given initial position of V, the initial position of AV falls in the shaded region, then the motion of the V–AV pair will be finite

separation of a finite motion. Two last assertions are equivalent and can be written as $R_a > \bar{\gamma} R_v$. Thus, the condition for finiteness of the motion of the V–AV pair at $L < 0$ is the simultaneous fulfilment of two conditions

$$\begin{cases} \lambda_{c2} < \lambda < 0, \\ R_a > \bar{\gamma} R_v. \end{cases} \quad (17)$$

The curve $\lambda = \lambda_{c2}$ is shown in Fig. 5 by a bold line.

In this case, the region $\lambda_{c2} < \lambda < 0$ is composed from two parts: the internal region bounded by the internal bold line and the circle $\rho = 1$, which corresponds to $\lambda = 0$, and the shaded external region. But the inequality $R_a > \bar{\gamma} R_v$ is satisfied only for the external part. The bold dotted line in this figure shows the curve $\lambda = \lambda_{c1}$ which is presented in Fig. 4 in more details. Thus, the relative position of V and IV determines the region of finiteness, where AV should be placed (at the given position of V relative to IV) in order that the motion of the V–AV pair be finite. The region of finiteness in Fig. 5 is shaded.

4. Conclusion

The condition of finiteness of the motion of the V–AV pair is the fulfilment of one of conditions (15) and (17). Each of these conditions, being true at the initial time moment, remains valid at any time moment of the dynamics. At a finite motion, V and AV move in the limits of concentric nonoverlapping rings (see Fig. 2, c, f). The sizes of these rings are determined by the product EL (see Fig. 3). If condition (15) is satisfied, the ring, where AV moves, is positioned inside of the ring, where V moves. If condition (17) is satisfied, the situation is

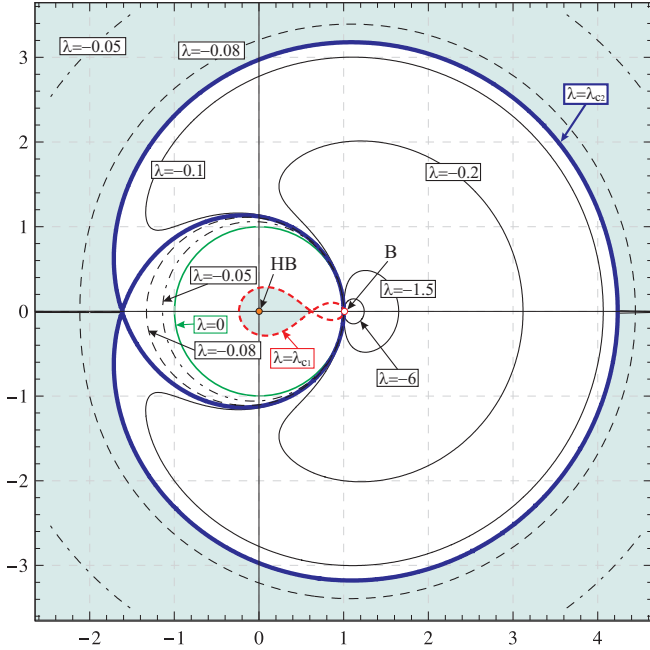


Fig. 5. Ratio $\rho(\Psi)$ given in (16) for various negative values of the parameter λ and for $\lambda = \lambda_{c1}$. If, at a given initial position of V, the initial position of AV falls in the shaded region, then the motion of the V–AV pair will be finite. The length unit is R_v

opposite. The graphic interpretation of conditions (15) and (17) is shown in Fig. 5: if, at the given initial position of V relative to IV, AV falls in the shaded region, then the motion of the V–AV pair will be finite.

The infinite motion of the V–AV pair at large distances from IV has the following characteristics: (i) velocities of V and AV tend to constant values $\dot{R}_v, \dot{R}_a \rightarrow \sqrt{E}$, and $\dot{\Phi}_v, \dot{\Phi}_a \rightarrow 0$; (ii) the distance between V and AV also tends to a constant $d \rightarrow 1/\sqrt{E}$.

The calculation in the present work was performed in the case of an unbounded magnet. But since the V–AV pair is a *localized* perturbation [25, 26], the effect of boundary conditions on the dynamics of the V–AV pair will be significant in the case of a particle with finite sizes only if the pair approaches the lateral surface of a magnetic at a distance comparable with d . Therefore, for particles with size larger than the distance between V and AV, the criterion of separation of the finite and infinite motions (15) can be considered as the estimation criterion of separation of the modes of annihilation of AV and IV and self-annihilation of the V–AV pair. For small-size particles, the mentioned criterion is inapplicable, and it is expedient to consider, in this case, the effect of the edge surface within the model of fixed boundary conditions [7, 28, 29]

The author is grateful to D.D. Sheka and Yu.B. Gaididei for the useful discussions. The present work is partially supported by the special program “Fundamental properties of physical systems under extreme conditions”, and by Deutsches Zentrum für Luft- und Raumfahrt e.V., Int. Büro d. BMBF, project No. UKR 08/001.

1. S.A. Wolf *et al.*, Science **294**, 1488 (2001).
2. S.D. Bader, Surface Science **500**, 172 (2002).
3. R. Skomski, J. Phys.: Condens. Matter. **15**, R841 (2003).
4. A. Hubert and R. Schäfer, *Magnetic Domains: the Analysis of Magnetic Microstructures* (Springer, Berlin, 1998).
5. T. Shinjo *et al.*, Science **289**, 930 (2000).
6. A. Wachowiak *et al.*, Science **298**, 577 (2002).
7. K.L. Metlov, K.Yu. Guslienko, J. Magn. Magn. Mater. **242-245**, 1015 (2002).
8. V.P. Kravchuk, D.D. Sheka, and Yu.B. Gaididei, J. Magn. Magn. Mater. **310**, 116 (2007).
9. R. Höllinger, A. Killinger, and U. Krey, J. Magn. Magn. Mater. **261**, 178 (2003).
10. S.D. Bader, Rev. Mod. Phys. **78**, 1 (2006).
11. B.A. Ivanov and G.M. Wysin, Phys. Rev. B **65**, 134434 (2002).
12. R. Hertel, S. Gliga, M. Fähnle, and C.M. Schneider, Phys. Rev. Lett. **98**, 117201 (2007).
13. B. Waeyenberge *et al.*, Nature **444**, 461 (2006).
14. K. Yamada *et al.*, Nature Mater. **6**, 270 (2007).
15. J.-G. Caputo, Yu.B. Gaididei, F.G. Mertens, and D.D. Sheka, Phys. Rev. Lett. **98**, 056604 (2007).
16. V.P. Kravchuk, D.D. Sheka, Yu.B. Gaididei, and F.G. Mertens, J. Appl. Phys. **102**, 043908, (2007).
17. S.-K. Kim, K.-S. Lee, Y.-S. Yu, Y.-S. Choi, Appl. Phys. Lett. **92**, 022509 (2008).
18. L. Landau and E. Lifshitz, Phys. Zs. Sowjet. **8**, 153 (1935).
19. A.M. Kosevich, B.A. Ivanov, and A.S. Kovalev, *Nonlinear Waves of Magnetization. Dynamical and Topological Solitons* (Naukova Dumka, Kyiv, 1983) (in Russian).
20. G. Gioia and R.D. James, Proc. R. Soc. Lond. A **453**, 213 (1997).
21. R. Rajaraman, *Solitons and Instantons. An Introduction to Solitons and Instantons in Quantum Field Theory* (North-Holland, Amsterdam, 1982).

22. A.R. Völkel, G.M. Wysin, F.G. Mertens, A.R. Bishop, and H.J. Schitzer, *Phys. Rev. B* **50**, 12711 (1994).
23. A.A. Thiele, *Phys. Rev. Lett.* **30**, 230 (1973).
24. D.L. Huber, *J. Appl. Phys.* **53**, 1899 (1982).
25. S. Komineas and N. Papanicolaou, in *Electromagnetic, Magnetostatic, and Exchange-Interaction Vortices in Confined Magnetic Structures*, edited by E.O. Kamenetskii (Research Signpost, Trivandrum, 2008).
26. N. Papanicolaou and P.N. Spathis, *Nonlinearity* **12**, 285 (1999).
27. S. Komineas and N. Papanicolaou, *New J. of Physics* **10**, 043021 (2008).
28. Yu.B. Gaididei, V.P. Kravchuk, F.G. Mertens, and D.D. Sheka, *Fiz. Nizk. Temp.* **34**, 669 (2008).
29. B.A. Ivanov and C.E. Zaspel, *Phys. Rev. Lett.* **99**, 247208 (2007).

Received 10.04.09.

Translated from Ukrainian by V.V. Kukhtin

ДИНАМІКА ПАРИ ВИХОР-АНТИВИХОР
У ПРИСУТНОСТІ НЕРУХОМОГО ВИХОРОУ
У ДВОВИМІРНОМУ ФЕРОМАГНЕТИКУ

В.П. Кравчук

Резюме

У двовимірному феромагнетику теоретично досліджено динаміку вихор-антивихрової пари в присутності нерухомого вихору. Розрахунки проведено в рамках моделі колективних змінних. Отримано критерії для початкових умов, що дозволяють розділити фінітний та інфінітний рух пари. Досліджено загальні характеристики кожного з типів рухів.